

Dynamic Obstacles Tracking in mmWave Networks

Rathindra Nath Dutta, Subhojit Sarkar and Sasthi C. Ghosh

Advanced Computing and Microelectronics Unit, Indian Statistical Institute, Kolkata, India

Abstract—The advent of fifth generation communication networks has led to novel opportunities and problems that were absent in legacy networks. Stringent line-of-sight demands necessitated by fast attenuating nature of millimeter waves (mmWave) through obstacles, pose to be one of the central problems of the field. mmWave links are easily disrupted due to obstacles, both static and dynamic. Handling static obstacles is easy, while dynamic obstacles are usually tracked by expensive additional hardware like cameras and radars, which undoubtedly lead to increased deployment costs. In this manuscript, we propose a novel approach to estimate the trajectories of multiple dynamic obstacles in an ultra dense mmWave network, solely based on link failure information, without resorting to any specialized tracking hardware. We keep a track of link failures over a short window of time and use that knowledge to extrapolate the trajectories of dynamic obstacles. After proving its NP-completeness, we employ a greedy set cover based approach for this. We then use the obtained trajectories to tag upcoming links as per their blockage possibility. We simulate on real world data to validate our approach based on its accuracy, sensitivity, and precision. Our approach is also shown to outperform an existing one.

Index Terms—Millimeterwaves, device to device, dynamic obstacles, obstacle tracking, ultra dense networks, greedy set cover

I. INTRODUCTION

The skyrocketing usage in internet-enabled handheld devices and their bandwidth hungry applications promise to drain the scant traditional spectrum that remains. The high bandwidth provided by millimeter wave (mmWave) communication, coupled with its relatively unused spectrum, makes it an attractive candidate to cater to such demand. Indeed, compared to traditional sub-6 GHz systems, the mmWave spectrum promises to provide multiple orders of magnitude increase in data rates, of upto several gigabits per second. mmWaves have rather short wavelengths, in the order of millimeters. As a result, they suffer from extremely high attenuation even through free space. Through obstacles, their attenuation is even worse. As a result, communication using mmWaves is usually viable only over very short distances, that too if there exists a line of sight (LOS) path between the communicating devices. Both static and dynamic obstacles can obstruct mmWave links. Static obstacles include man-made structures such as buildings, bridges, signboards, and natural obstruction like trees, bushes. Detecting static obstacles on the transmission path is a comparatively easier task; typically such data is stored at the base station (BS) using satellite data, or open source maps [1]. Several methods have been proposed that allocate links avoiding these static obstacles [2], [3].

Dynamic obstacles on the other hand pose a harder problem; the continuously changing dynamic environment presents a

unique challenge to the problem of mmWave link allocation. Dynamic obstacles obstructing mmWaves include pedestrians and vehicles. It has been found out that human blockages cause upto a 20-30 dB attenuation [4], while for a tinted car window the attenuation is 30-35 dB [5]. Such obstruction causes intermittent outages, decay in system throughput, and degrades overall user experience. Additionally, a number of unnecessary handovers are often introduced because of dynamic obstacles [6], which further add to system overhead. As such, dealing with dynamic obstacles in an mmWave network forms a key challenge. One way to deal with dynamic obstacles is via multi-connectivity [7]. Here, multiple BSs have to be involved, some kept as backup as a precautionary measure for possible link failure, a process which wastes precious resources. There have also been approaches that assume a fixed distribution of blockage probabilities due to dynamic obstacles; for example, in [8], the authors use this assumption for stable resource allocation. However, neither of these approaches effectively tracks dynamic obstacles.

The classical way to actively track dynamic obstacles is by deploying additional hardware. In fact, hardware dependent dynamic obstacle tracking is well-studied. Usual hardware used for tracking include LiDARs [9]–[12], cameras [4], [13]–[22], and lasers [23]–[25]. The primary drawback of deploying such additional hardware is the considerable cost overhead that has to be borne by the service providers, and subsequently by the end users. Indeed, hardware such as radars are quite expensive and are sometimes prohibitive for ubiquitous deployment. Cameras on the other hand introduce privacy concerns [26], along with considerable image processing overhead.

In this manuscript, we propose an approach to the problem of tracking dynamic obstacles in an mmWave network, without using any additional hardware such as camera, radar, or LiDAR. Given usual baseline infrastructure and historical link failure information, we attempt to obtain the trajectories of dynamic obstacles, and use them to predict blockage status of possible future links. Link failures have been previously used in [6] to track the location and trajectory of a user equipment (UE); the authors used a multi-armed bandit approach to achieve efficient handovers. For a given UE, they essentially used a signal space partitioning scheme based on its LOS information with the BSs. Motivated by their idea, we attempt to use historical link failure data to straightaway track the dynamic obstacles. The challenge lies in the fact that while UEs can report their spatiotemporal details to a BS, the same is not true for dynamic obstacles as they move independently outside the purview of the BS. The problem becomes even harder when considered without any additional tracking hard-

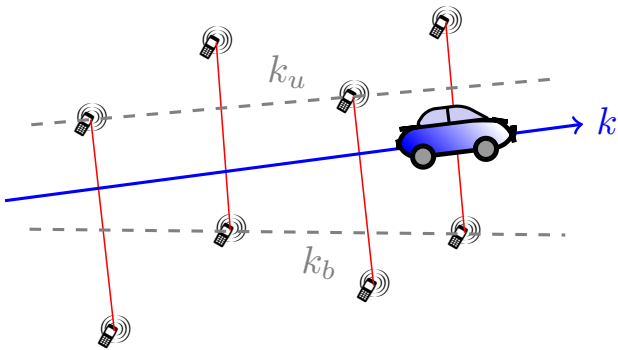


Fig. 1: A dynamic obstacle blocking a few links

ware to obtain such details. To the best of our knowledge, there exists no previous work that attempts to deal with the dynamic obstacle tracking problem (DOTP) in a mmWave network without resorting to additional tracking hardware. In this work, using the knowledge of past link failures, we try to obtain the possible obstacle trajectories. We emphasize here that exact path of a dynamic obstacle may not necessarily be required. Rather, a narrow region containing the actual trajectory may suffice to justify a given set of link failures. Such a narrow region, termed as *band* on the Cartesian plane, can be represented by its two extreme lines l_1 and l_2 as shown in Fig. 1. The black line segments represent the links broken by a car moving along a trajectory line k . We aim to obtain such a band for each dynamic obstacle trajectory. With enough historical link failure information the band becomes narrower, and thus every line contained in that band can be considered equivalent with respect to link failures.

More formally, our main contribution in this paper can be summarised as follows:

- We have embarked upon, what we believe, is the first attempt to track trajectories of multiple dynamic obstacles that obstruct LOS transmission in a mmWave network, without resorting to any additional tracking hardware like LiDARs, radars, or cameras.
- An integer linear program (ILP) is developed for the dynamic obstacle tracking problem, and the problem is proved to be NP-complete.
- We provide a greedy set cover based algorithm to obtain the trajectories of dynamic obstacles.
- We validate our proposed approach through simulation using the San Francisco taxi dataset [27].
- We compare our proposed approach with existing baseline approaches, and show that our approach significantly minimizes link failures.

The rest of this manuscript is arranged as follows. We detail our considered system model in Section II. Section III provides the problem formulation followed by its hardness proof. A greedy solution is given in IV, followed by its simulation results in Section V. We conclude this work with Section VI.

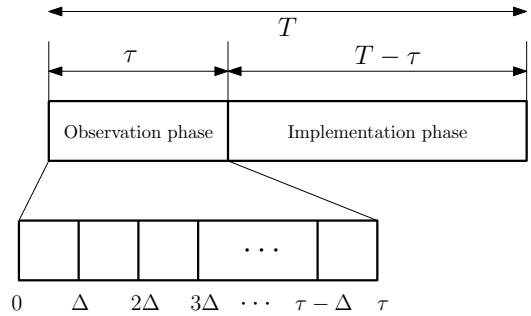


Fig. 2: A time epoch T

II. SYSTEM MODEL

We consider an urban service area having a central BS, and a few small cell mmWave base stations (gNBs) distributed uniformly at random within the service area. We discretize the time into slots $0, \Delta, 2\Delta, \dots$, where each slot is of duration Δ . We consider there are some mmWave communications happening all over the service area. At each time slot t , we consider the set of active mmWave links to be \mathcal{L}_t ; each such link can be either a device-to-device (D2D) link between two UEs, or a link between a UE and a gNB. Each link can be represented by a line segment as the location information of the communicating devices forming the link are available at the central BS.

a) *Obstacle Modelling*: Since the static obstacles have fixed location and sizes, their spatial information can be acquired by the BS from open source maps like OpenStreetMaps [1]. Therefore, we assume that the mmWave links are allocated by avoiding static obstacles by relying via other UEs [3], or reflecting surfaces [2]. Since primary focus of this work is to track the dynamic obstacles from past link failures, we assume that link failures occur due to the presence of dynamic obstacles only. We ignore the other possible causes of link failures such as imperfect channel state information or high interference from neighbouring UEs. Let $\mathcal{L}_t^B \subseteq \mathcal{L}_t$ denote the set of such blocked links at time t . We assume that obstacles move along a straight line for a small time epoch T . This is a reasonable assumption, since for example, a car changes directions rather infrequently, and T is a small period in the order of few seconds.

b) *Discovery and Implementation Phases*: Each time epoch T is divided up into two phases, namely the *discovery* phase of duration τ , and the *implementation* phase of remaining duration $T - \tau$ as shown in Fig. 2. At the end of the discovery phase, we utilize the past link failure information available to figure out the possible obstacle trajectory bands, which are then used to predict potential link failures in the implementation phase. After each time epoch T , the process starts afresh.

III. PROBLEM FORMULATION

Let \mathcal{L} be the set of all blocked links, that is $\mathcal{L} = \bigcup_t \mathcal{L}_t^B$. Note that $K = \max_t \{|\mathcal{L}_t^B|\}$ represents an upper bound on the

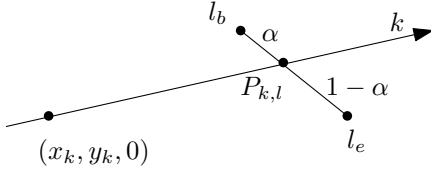


Fig. 3: Intersection of line k with link l at point $P_{k,l}$

number of dynamic obstacles moving in the area, as each link may be blocked by different obstacles. In order to write the considered DOTP in a mathematical form, we introduce a set of binary indicator variables $X_k \in \{0, 1\}$ for all $0 \leq k \leq K$ defined as follows:

$$X_k = \begin{cases} 1 & \text{when obstacle } k \text{ causes at least one link failure} \\ 0 & \text{otherwise} \end{cases}$$

Now, our objective is to find the minimum number of obstacles accounting for all link failures. Thus, the objective function can be given by:

$$\text{minimize} : \sum_{k=1}^K X_k \quad (1)$$

Now let us introduce another set of binary indicator variables $Y_{k,l} \in \{0, 1\}$ for all $1 \leq k \leq K$ and $1 \leq l \leq |\mathcal{L}|$ defined as follows:

$$Y_{k,l} = \begin{cases} 1 & \text{when } l\text{-th link is failed due to } k\text{-th obstacle} \\ 0 & \text{otherwise} \end{cases}$$

Clearly we need to have,

$$\sum_{k=1}^K Y_{k,l} \geq 1 \quad \forall l \quad (2)$$

At time instant t , a link l is failed due to an obstacle k , only if the trajectory line of obstacle k intersects the line segment representing the link. For notational brevity, from now onward we refer to the trajectory of obstacle k and the line segment representing the link l simply by the indices k and l respectively. A link l is defined by its two end points l_b and l_e . Now an obstacle k intersects a link l at point $P_{k,l}$ if and only if k partitions the line segment l in the ratio $\alpha_{k,l}$ and $1 - \alpha_{k,l}$, where $0 \leq \alpha_{k,l} \leq 1$ as shown in Fig. 3. The coordinate of $P_{k,l}$ can be computed from l and $\alpha_{k,l}$ as follows.

$$P_{k,l}[x] = \alpha_{k,l}l_b[x] + (1 - \alpha_{k,l})l_e[x] \quad (3)$$

$$P_{k,l}[y] = \alpha_{k,l}l_b[y] + (1 - \alpha_{k,l})l_e[y] \quad (4)$$

$$P_{k,l}[t] = t \text{ such that } l \in \mathcal{L}_t \quad (5)$$

Here for a point P , $(P[x], P[y])$ denotes its spatial coordinates on the Cartesian plane, and $P[t]$ denotes the time when this point on the link l is being considered, thus a constant for a link l . Now the intersection point $P_{k,l}$ must also lie on the trajectory line k , and it must therefore satisfy the equation of the line k given by

$$\frac{x - x_k}{\delta x_k} = \frac{y - y_k}{\delta y_k} = \frac{t - 0}{\delta t_k}$$

Here $(x_k, y_k, 0)$ is the initial point on the line k at time $t = 0$. The parameters $\delta x_k, \delta y_k$ and δt_k are the intercept values with x, y and t axes respectively. Thus, we have $x = x_k + t \frac{\delta x_k}{\delta t_k}$ and $y = y_k + t \frac{\delta y_k}{\delta t_k}$. Since for a line, $\frac{\delta x_k}{\delta t_k}$ and $\frac{\delta y_k}{\delta t_k}$ are constants, they can be dealt with only two variables, namely A_k and B_k respectively, in our mathematical program. Thus, whether the point $P_{k,l}$ lies on the line k or not, can be encoded by the following linear constraints $\forall k, l$:

$$P_{k,l}[x] = x_k + P_{k,l}[t] A_k \quad (6)$$

$$P_{k,l}[y] = y_k + P_{k,l}[t] B_k \quad (7)$$

Note that here, $P_{k,l}[t] = t$, is a constant specified by the link k as mentioned above. Now combining (3) with (6) and (4) with (7) we have the following two linear constraints:

$$\alpha_{k,l}l_b[x] + (1 - \alpha_{k,l})l_e[x] = x_k + P_{k,l}[t] A_k \quad (8)$$

$$\alpha_{k,l}l_b[y] + (1 - \alpha_{k,l})l_e[y] = y_k + P_{k,l}[t] B_k \quad (9)$$

Note here $\alpha_{k,l}, x_k, y_k, A_k, B_k$ all are optimization variables and the rest are constants. We must also ensure $0 \leq \alpha_{k,l} \leq 1$ whenever $Y_{k,l} = 1$. This can be encoded as a linear constraint by introducing a large positive constant M , denoting positive infinity as follows:

$$-(1 - Y_{k,l})M \leq \alpha_{k,l} \leq 1 + (1 - Y_{k,l})M \quad (10)$$

The integrality constraints are given by

$$X_k, Y_{k,l} \in \{0, 1\} \quad (11)$$

Thus the ILP is given by the objective function (1) and constraints (2), (8), (9), (10) and (11).

We next prove that the problem of detecting multiple obstacle trajectories is NP-complete.

Lemma 1. *DOTP is NP-complete.*

Proof. To show that DOTP is NP-complete, we choose the point-line-cover (PLC) [28] problem as the candidate for reduction. In PLC, given n points and an integer k , we need to decide whether there exists k - straight lines such that all points are covered. Here, a line l is said to cover a point p if and only if p lies on l . PLC is a known NP-complete problem [28]. Given an instance $I = (P = \{p_1, p_2, \dots, p_n\}, k)$ of PLC, we apply the following reduction. For every point $p_i \in P$, we create two points p'_i and p''_i , both having co-ordinates same as that of p_i . Moreover, (p'_i, p''_i) forms a link of zero length at time t_i for our DOTP. Now suppose, there exists a deterministic polynomial time algorithm \mathcal{A} for DOTP. Then for a given instance $I' = (\mathcal{L} = \{\mathcal{L}_{t_i} = \{(p'_i, p''_i) \mid p_i \in P\}\}, k)$ of DOTP, \mathcal{A} decides in polynomial time whether there exist k lines such that all links are intersected by at least one of these lines. Now by construction, if a line intersects a link (p'_i, p''_i) , it must also cover the original point p_i in PLC, and vice versa. This means we have essentially solved instance I of PLC in polynomial time. This is a contradiction. Therefore, DOTP is NP-hard, and such an algorithm \mathcal{A} cannot exist unless P=NP.

Now to show DOTP is also in NP, consider the fact that given k obstacle trajectories (lines), one can easily verify

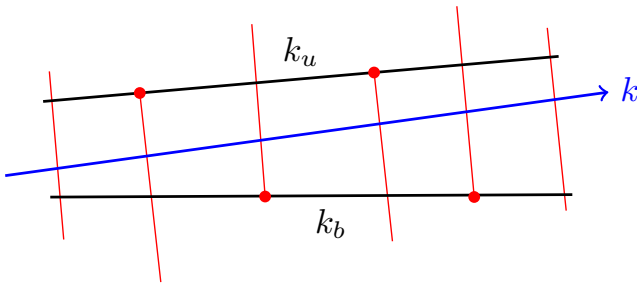


Fig. 4: A band for a set of blocked links

whether all links are blocked (intersected) by at least one of them. Thus, DOTP is NP-complete. \square

IV. DISCOVERY AND IMPLEMENTATION ALGORITHMS

As mentioned in Section II, our approach works in two phases. While in the discovery phase we try to obtain the possible trajectory bands of the dynamic obstacles, in the implementation phase we apply this knowledge to tag the future link requests as per their blockage estimates. Next we present a greedy algorithm to obtain these obstacle trajectory bands \mathcal{O} , followed by a simple tagging scheme to mark future links in implementation phase for potential blockages.

A. Dynamic Obstacle Tracking Algorithm

We can model DOTP as a set cover problem as follows. Suppose we are given some candidate trajectory lines, each covering a subset of the universe \mathcal{L} . A trajectory line k covers a link $l \in \mathcal{L}$ if k intersects the link l . Then an optimal (minimum) set cover of this, essentially gives us the required solution of the DOTP. Recall that the set cover problem is a well known APX-hard problem [29]. A greedy solution to set cover can be obtained by repeatedly selecting the set covering maximal number of yet to be covered elements. It can be shown that this approach has an approximation ratio of $\log n$, where n is the number of candidate sets. Thus given a set of possible trajectory lines, we already have an approximation algorithm that returns a minimal subset of trajectory lines covering all links.

The main challenge is to get this set of candidate trajectory lines, as there can be infinitely many possible lines intersecting two or more links. Now observe the following interesting fact. Whenever a line k covers a set of links $\mathcal{L}_k \subseteq \mathcal{L}$ by intersecting all of them, there must exist a band such that all lines falling inside that band also covers \mathcal{L}_k as depicted in Fig. 1. Given a trajectory line k and its associated set \mathcal{L}_k , band for k is defined by two boundary lines k_u and k_b , where each boundary line is uniquely defined by two end points of two different links in \mathcal{L}_k as depicted in Fig 4.

As mentioned earlier, the bands become narrower with the increase in available link failure information. Thus we can treat a trajectory line k and its corresponding band equivalently, with respect to the link failures. Therefore, it suffices to report only these bands defined by its two boundary lines. Now note

that, the same band can correspond to all possible trajectories that intersects the same set of links in \mathcal{L}_k . However, given a trajectory line k , we can uniquely obtain its corresponding band defined by its two boundary lines k_u and k_b from \mathcal{L}_k . Thus reporting any line contained in a band is equivalent to reporting the entire band. Now observe that, both k_u and k_b can serve as such a line. This observation actually gives us a way to obtain the candidate trajectory sets. If we consider the set \mathcal{S} of lines passing through the end point pairs of all possible links, all the required trajectory lines must be a subset of \mathcal{S} . Moreover the solution must be the minimum subset of \mathcal{S} covering entire \mathcal{L} . Since for two links l and l' , there are four possible pairings, namely (l_b, l'_b) , (l_b, l'_e) , (l_e, l'_b) and (l_e, l'_e) . Thus there are at most $4 \binom{|\mathcal{L}|}{2}$ end point pairs, the size of \mathcal{S} is finite and is in the order of $O(|\mathcal{L}|^2)$. Furthermore, we can reduce the search space to only $2 \binom{|\mathcal{L}|}{2}$, since obtaining both k_u and k_b for a trajectory line k is redundant, only one of them would suffice. Given a line $k \in \mathcal{S}$ joining two end points of two links from \mathcal{L} , we scan the entire \mathcal{L} , to find how many links are intersected by this line k , which gives us the set $\mathcal{S}_k \subseteq \mathcal{L}$, the set of links covered by this line. This can be computed in linear time with respect to \mathcal{L} . Once we obtain all such \mathcal{S}_k , we follow the footsteps of greedy set cover solution described above. This will return us at most $OPT \times \log(|\mathcal{L}|)$ many trajectories where OPT is the size of optimal set cover solution. This process is formalized into Algorithm 1. The overall running time of this $O(|\mathcal{L}|^4)$.

Algorithm 1: Set Cover Based DOTP

```

1 Set  $\mathcal{U} \leftarrow \mathcal{L}$  // universe to cover
2 Set  $\mathcal{S} \leftarrow \emptyset$  // candidate trajectories
3 Set  $\mathcal{O} \leftarrow \emptyset$  // output trajectories
  /* generating candidate lines */
4 for  $l \in \mathcal{L}$  do
5   for  $l' \in \mathcal{L}$  and  $l \neq l'$  do
6      $k \leftarrow (l_b, l'_b)$  // pair of link endpoints
7      $k' \leftarrow (l_b, l'_e)$ 
8      $\mathcal{S} \leftarrow \mathcal{S} \cup \{k, k'\}$ 
  /* apply greedy set cover */
9 while  $\mathcal{U} \neq \emptyset$  do
10  for  $k \in \mathcal{S}$  do
11     $C_k \leftarrow \{l \in \mathcal{U} \mid \text{intersection}(k, l) = 1\}$ 
12     $k \leftarrow \underset{k' \in \mathcal{S}}{\text{argmax}} \{C_{k'}\}$ 
13     $\mathcal{U} \leftarrow \mathcal{U} \setminus C_k$ 
14     $\mathcal{O} \leftarrow \mathcal{O} \cup \{k\}$ 
15 return  $\mathcal{O}$ 

```

B. Link Tagging Algorithm

Post the discovery phase τ , our greedy Algorithm 1 computes and returns \mathcal{O} , the minimal set of candidate lines which covers all broken links in \mathcal{L} . Using this information, we allocate links in the implementation phase, i.e., in the $T-\tau$

remaining time in an epoch T . We have a set \mathcal{F} of future link requests, which we want to test for possible future blockage. We activate only those links that would not be blocked by the obstacles given by \mathcal{O} . In other words, for a requested link l , we tag l as “free” only if it does not get obstructed by any obstacle, that is both l_b and l_e are on the same side of each line in \mathcal{O} . Therefore, we initially tag each requested link as “free”, and if any link intersects with a line in \mathcal{O} we change its tag to “blocked”. This tagging procedure is formalized into Algorithm 2.

Notice that in both Algorithms 1 and 2, we are required to test whether a line k intersects a link l . Next we describe an efficient procedure for this.

Algorithm 2: Link Tagging Algorithm

```

1 for  $l \in \mathcal{F}$  do
2   Mark  $l$  as “free”
3   for  $k \in \mathcal{O}$  do
4     if  $\text{intersection}(k, l) = 1$  then
5       Mark  $l$  as “blocked”

```

The $\text{intersection}(k, l)$ Procedure:

Now recall that a line k is uniquely defined by two points on it and the line segment defined by the two end points l_b and l_e for a link l . Now a link l intersects with the line k if and only if l_b and l_e lie on the two opposite sides of k as shown in Fig. 3. Let the line equation of k be written as $f_k(x, y) = 0$ form. Now observe that if we put the coordinates of l_b and l_e into the line equation of k , it would give opposite signs if and only if they lie on different sides of line k . This provides us an efficient way to test for intersection: k intersects l if and only if $f_k(l_b) \times f_k(l_e) \leq 0$. The subroutine returns 1 in there is an intersection, 0 otherwise.

V. SIMULATION RESULTS

To validate the performance of our proposed approach, we run simulations using the CRAWDA taxi dataset [27], which contains GPS taxi traces in San Francisco Bay Area, USA. We randomly select 15 taxis from this dataset as our dynamic obstacles, and run our experiments. We consider a set of link requests generated uniformly at random over the service area, for the considered time period epoch $T = 12$. We execute Algorithm 1 on the blocked links generated upto time τ . Thereafter, we run Algorithm 2 for the requests generated after τ , and tag each such requested link accordingly. We measure the performance of our tagging scheme based on three metrics, namely *accuracy*, *precision*, and *sensitivity*, which are defined as follows.

- *accuracy*: the ratio of number of links correctly tagged according to their blocking status, to the total number of links under consideration.
- *sensitivity*: ratio of the number of links correctly tagged as “blocked”, to the total number of actually blocked links.

- *precision*: ratio of the number of links correctly tagged as “blocked”, to the number of links correctly tagged as “blocked” plus the number of links incorrectly tagged as “blocked”.

We vary the duration of discovery phase τ from 5 to 10 seconds, and plot these three metrics in Fig. 5 for different number of obstacles and link requests. As is intuitive, all three metrics see an improvement with increase in discovery phase time τ . Furthermore, increasing the number of obstacles from 5 to 10 as well as the number of link requests from 500 to 1000 in the discovery phase lead to higher number of link failures, giving us more information to more accurately track the obstacles. This is reflected for all three metrics as evident in Fig. 5. Note that we use the symbol # to denote the phrase ‘number of’.

Next, we compare the performance of our Proposed methodology with two baseline approaches. For the first one, we consider no information about dynamic obstacles is available at the BS; we refer to this approach as Zero. We also consider a fixed distribution of blockage probabilities based approach as considered in [8] and we call this Fixed. In Fig. 6(a), for a fixed number (500) of link requests, we vary the number of dynamic obstacles from 4 to 14, and plot the number of link failures for all three considered approaches. Here we assume that all the link requests can be activated simultaneously, and we activate only those links that are tagged as “free”. In case of Fixed scheme, for each requested link, we generate a number p uniformly at random in the closed interval $[0, 1]$, and we activate the link only if p is less than the probability of the link not being blocked. As is intuitive, Zero performs the worst, followed by Fixed, and Proposed. Also, increase in obstacle count leads to more frequent failures as expected.

A similar effect is observed when we fix the number of dynamic obstacles at 10, and vary the number of link requests from 500 to 1000. In Fig. 6(b), we see that the link failure increases with the number of link requests as one would expect. Our Proposed approach performs the best, followed by Fixed and Zero.

VI. CONCLUSION AND FUTURE DIRECTION

In this manuscript, we have proposed a link failure based dynamic obstacle tracking approach, without resorting to expensive hardware like cameras and radars. We have proved the hardness of our problem, and have proposed an approximation algorithm based on set cover to solve it. The output of the algorithm is used to allocate better links in the future, leading to lesser link failures. The obvious drawback of this paper is that it needs dense user demand to extract dynamic obstacle trajectories; our approach will fail for sparse networks. In such sparse networks, our approach might need augmentation with some additional hardware, which can lead to new optimization problems. Another future direction can be doing away with the assumption that dynamic obstacles move in straight lines. Generalizing such trajectories to handle non-linear paths would give rise to newer challenges. Yet another

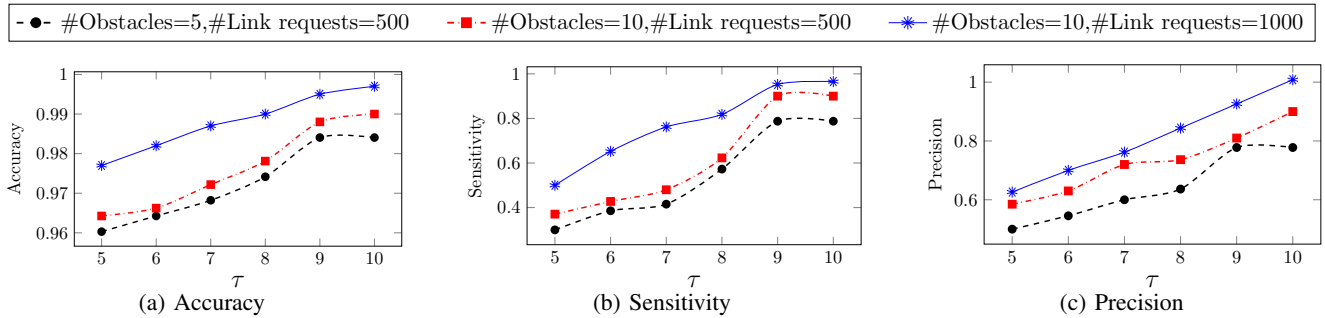


Fig. 5: Accuracy, Sensitivity and Precision vs. Discovery time τ for varying number of dynamic obstacles and link requests

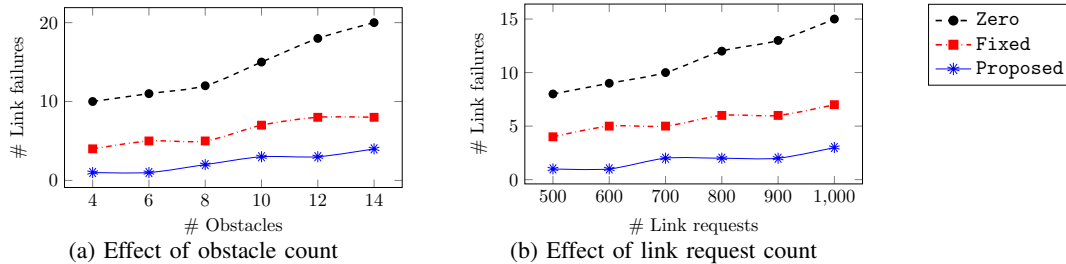


Fig. 6: Comparison of implementation phase performance

avenue of research may involve using trajectory data from our approach to deploy unmanned aerial vehicular base stations towards zones of future congestion. Lastly, in this work we have considered the information provided by historical link failures only, while historical link successes can also provide valuable information. In particular, using information about past link successes would intuitively give narrower bands, and will be explored in our future work.

REFERENCES

- [1] M. Haklay and P. Weber, "Openstreetmap: User-generated street maps," *IEEE Pervasive Computing*, vol. 7, no. 4, pp. 12–18, 2008.
- [2] E. Björnson, Ö. Özdoğan, and E. G. Larsson, "Reconfigurable intelligent surfaces: Three myths and two critical questions," *IEEE Commun. Mag.*, vol. 58, no. 12, pp. 90–96, 2020. [Online]. Available: <https://doi.org/10.1109/MCOM.001.2000407>
- [3] S. Sarkar and S. C. Ghosh, "Relay selection in millimeter wave D2D communications through obstacle learning," *Ad Hoc Networks*, vol. 114, p. 102419, 2021. [Online]. Available: <https://doi.org/10.1016/j.adhoc.2021.102419>
- [4] Y. Koda, K. Yamamoto, T. Nishio, and M. Morikura, "Reinforcement learning based predictive handover for pedestrian-aware mmwave networks," in *IEEE INFOCOM 2018 - IEEE Conference on Computer Communications Workshops (INFOCOM WKSHPs)*, 2018, pp. 692–697.
- [5] J. Jebramcik, J. Wagner, N. Pohl, I. Rolfes, and J. Barowski, "Millimeter wave material measurements for building entry loss models above 100 ghz," in *2021 15th European Conference on Antennas and Propagation (EuCAP)*, 2021, pp. 1–5.
- [6] L. Sun, J. Hou, and T. Shu, "Spatial and temporal contextual multi-armed bandit handovers in ultra-dense mmwave cellular networks," *IEEE Transactions on Mobile Computing*, vol. 20, no. 12, pp. 3423–3438, 2021.
- [7] M. Polese, M. Giordani, M. Mezzavilla, S. Rangan, and M. Zorzi, "Improved handover through dual connectivity in 5g mmwave mobile networks," *IEEE Journal on Selected Areas in Communications*, vol. 35, no. 9, pp. 2069–2084, 2017.
- [8] R. N. Dutta and S. C. Ghosh, "Mobility aware resource allocation for millimeter-wave D2D communications in presence of obstacles," *Comput. Commun.*, vol. 200, pp. 54–65, 2023. [Online]. Available: <https://doi.org/10.1016/j.comcom.2022.12.025>
- [9] D. Marasinghe, N. Rajatheva, and M. Latva-aho, "Lidar aided human blockage prediction for 6g," in *2021 IEEE Globecom Workshops (GC Wkshps)*, 2021, pp. 1–6.
- [10] S. Wu, C. Chakrabarti, and A. Alkhateeb, "Proactively predicting dynamic 6g link blockages using lidar and in-band signatures," 2022.
- [11] D. Marasinghe, N. Jayaweera, N. Rajatheva, S. Hakola, T. Koskela, O. Tervo, J. Karjalainen, E. Tirola, and J. Hultkonen, "Lidar aided wireless networks - beam prediction for 5g," in *2022 IEEE 96th Vehicular Technology Conference (VTC2022-Fall)*, 2022, pp. 1–7.
- [12] D. Marasinghe, N. Rajatheva, and M. Latva-aho, "Lidar aided human blockage prediction for 6g," in *2021 IEEE Globecom Workshops (GC Wkshps)*, 2021, pp. 1–6.
- [13] Y. Oguma, R. Arai, T. Nishio, K. Yamamoto, and M. Morikura, "Proactive base station selection based on human blockage prediction using rgb-d cameras for mmwave communications," in *2015 IEEE Global Communications Conference (GLOBECOM)*, 2015, pp. 1–6.
- [14] Y. Koda, K. Nakashima, K. Yamamoto, T. Nishio, and M. Morikura, "Cooperative sensing in deep rl-based image-to-decision proactive handover for mmwave networks," in *2020 IEEE 17th Annual Consumer Communications & Networking Conference (CCNC)*, 2020, pp. 1–6.
- [15] G. Charan, M. Alrabeiah, and A. Alkhateeb, "Vision-aided 6g wireless communications: Blockage prediction and proactive handoff," *IEEE Transactions on Vehicular Technology*, vol. 70, no. 10, pp. 10193–10208, 2021.
- [16] M. A. L. Sarker, I. Orikumhi, J. Kang, H.-K. Jwa, J.-H. Na, and S. Kim, "Vision-aided beam allocation for indoor mmwave communications," in *2021 International Conference on Information and Communication Technology Convergence (ICTC)*, 2021, pp. 1403–1408.
- [17] Y. Oguma, T. Nishio, K. Yamamoto, and M. Morikura, "Performance modeling of camera-assisted proactive base station selection for human blockage problem in mmwave communications," in *2016 IEEE Wireless Communications and Networking Conference*, 2016, pp. 1–7.
- [18] M. Alrabeiah, A. Hredzak, and A. Alkhateeb, "Millimeter wave base stations with cameras: Vision aided beam and blockage

- prediction,” *CoRR*, vol. abs/1911.06255, 2019. [Online]. Available: <http://arxiv.org/abs/1911.06255>
- [19] G. Charan, M. Alrabeiah, and A. Alkhateeb, “Vision-aided 6g wireless communications: Blockage prediction and proactive handoff,” *IEEE Transactions on Vehicular Technology*, vol. 70, no. 10, pp. 10193–10208, 2021.
- [20] Y. Koda, K. Nakashima, K. Yamamoto, T. Nishio, and M. Morikura, “Cooperative sensing in deep rl-based image-to-decision proactive handover for mmwave networks,” in *2020 IEEE 17th Annual Consumer Communications & Networking Conference (CCNC)*, 2020, pp. 1–6.
- [21] T. Nishio, H. Okamoto, K. Nakashima, Y. Koda, K. Yamamoto, M. Morikura, Y. Asai, and R. Miyatake, “Proactive received power prediction using machine learning and depth images for mmwave networks,” *IEEE Journal on Selected Areas in Communications*, vol. 37, no. 11, pp. 2413–2427, 2019.
- [22] G. Charan and A. Alkhateeb, “Computer vision aided blockage prediction in real-world millimeter wave deployments,” 2022.
- [23] M. Häselich, B. Jöbgen, N. Wojke, J. Hedrich, and D. Paulus, “Confidence-based pedestrian tracking in unstructured environments using 3d laser distance measurements,” in *2014 IEEE/RSJ International Conference on Intelligent Robots and Systems*, 2014, pp. 4118–4123.
- [24] S. Gidel, P. Checchin, C. Blanc, T. Chateau, and L. Trassoudaine, “Pedestrian detection and tracking in an urban environment using a multilayer laser scanner,” *IEEE Transactions on Intelligent Transportation Systems*, vol. 11, no. 3, pp. 579–588, 2010.
- [25] A. Fod, A. Howard, and M. Mataric, “A laser-based people tracker,” in *Proceedings 2002 IEEE International Conference on Robotics and Automation (Cat. No.02CH37292)*, vol. 3, 2002, pp. 3024–3029 vol.3.
- [26] A. T.-Y. Chen, M. Biglari-Abhari, and K. I.-K. Wang, “Context is king: Privacy perceptions of camera-based surveillance,” in *2018 15th IEEE International Conference on Advanced Video and Signal Based Surveillance (AVSS)*, 2018, pp. 1–6.
- [27] M. Piorkowski, N. Sarafijanovic-Djukic, and M. Grossglauser, “Crawdad epfl/mobility,” 2022. [Online]. Available: <https://dx.doi.org/10.15783/C7J010>
- [28] S. Kratsch, G. Philip, and S. Ray, “Point line cover: The easy kernel is essentially tight,” *ACM Trans. Algorithms*, vol. 12, no. 3, apr 2016. [Online]. Available: <https://doi.org/10.1145/2832912>
- [29] N. Alon, D. Moshkovitz, and S. Safra, “Algorithmic construction of sets for k-restrictions,” *ACM Trans. Algorithms*, vol. 2, no. 2, p. 153–177, apr 2006. [Online]. Available: <https://doi.org/10.1145/1150334.1150336>